Development and Validation of a Toddler Manikin for Assessing Belt Fit in Aviation Seat

Matthew P. Reed
Sheila M. Ebert
Kyle J. Boyle

University of Michigan Transportation Research Institute

December 2017

UNIVERSITY OF MICHIGAN
TRANSPORTATION
RESEARCH INSTITUTE
UNIVERSITY OF MICHIGAN

Technical Report Documentation Page

1. Report No. UMTRI-2017-7	2. Government Accession No.	3. Recipient's Catalog No.
4. Title and Subtitle Development and Validation of a Toddler Manikin for Assessing Belt Fit in Aviation Seats		5. Report Date December 2017
		6. Performing Organization Code
7. Author(s) Reed, Matthew P., Ebert, Sheila M., and Boyle, Kyle J.		8. Performing Organization Report No.
9. Performing Organization Name and Address University of Michigan Transportation Research Institute 2901 Baxter Rd. Ann Arbor MI 48109		10. Work Unit No. (TRAIS)
		11. Contract or Grant No. FAA Grant 16-G-010
12. Sponsoring Agency Name and Address Federal Aviation Administration		13. Type of Report and Period Covered
		14. Sponsoring Agency Code
15. Supplementary Notes		

16. Abstract

No standardized procedure or tool currently exists for measuring belt fit for children in aviation seats. A belt fit test manikin representing a typical two-year-old child in the U.S. was developed to address the smallest passengers for whom the lap belt is intended to be functional. The manikin external contours were based on the output of a statistical analysis of child body shape and constructed from ABS using additive manufacturing techniques. A metal linkage was constructed that provides appropriate mass and mobility in the neck and hips. A validation study was conducted using thirty-eight child volunteers. Lap belt fit was measured in adult- and child-selected postures and at three lap belt angles. Additional measurements were obtained with the child wearing a CARES harness, the only add-on harness currently approved for use in aviation seats. Extensive anthropometric data were obtained from the participants, including three-dimensional whole-body surface scans. Statistical analysis revealed significant effects of lap belt angle on the placement of the lap belt with respect to the pelvis, but differences between adult- and child-selected postures were not significant due to large variability. For most children and conditions, the lap belt overlaid the pelvis. Body size was only weakly related to lap belt fit, with larger children experiencing lap belt fit that was lower and further rearward (closer to the pelvis). However, only about 10% of the variation in lap belt positioning was attributable to child body size. The manikin belt fit measures were directionally consistent with the effects of lap belt angle on child belt fit. On average, the manikin belt fit was closer to the pelvis (lower and more rearward) than was the case for children. Using the demonstrated relationship between manikin and child belt fit, the manikin and associated procedure can be used to assess belt fit in aviation seats.

17. Key Words children, anthropometry, aviation seats, posture, belt fit	18. Distribution Statement		
19. Security Classif. (of this report)	20. Security Classif. (of this page)	21. No. of Pages 46	22. Price

Form DOT F 1700.7 (8-72)   Reproduction of completed page authorized

ACKNOWLEDGMENTS

CONTENTS

INTRODUCTION

Proper belt fit is a pre-requisite for good occupant protection in aviation seats. Most aviation seats are provided with only a lap belt, and protecting the smallest occupants is a particular challenge because the immature pelvis of a child provides a small target for the belt. The U.S. Federal Aviation Administration mandates that belts should fit a range of occupants from large men to children as small as two years of age. A suitable surrogate to evaluate the belt fit for the smallest occupants does not currently exist. To assess belt fitment, seat manufacturers currently place a child approximately two years of age into the seat. Due to differences in child body dimensions and posture, this procedure lacks objectivity and reproducibility.

To address this need, a research program was initiated to develop a manikin and measurement procedures to assess belt fit in aviation seats. A series of previous studies have addressed restraint fit, including belt and harness fit for children (Reed et al. 2008a, b; Reed et al. 2013). These studies have led to the development of standardized procedures for positioning anthropomorphic test devices (ATDs) representing children and conducting repeatable and reproducible assessments of belt fit with and without boosters that can be linked to belt fit on children (Reed et al. 2009). However, no currently available ATD is the size of a typical two-year-old (2YO) child, and the available ATDs lack realistic body contours.

Over the past 5 years, several detailed studies of child body shape have been conducted, measuring hundreds of children ages 1 to 12 years using laser and optical scanners (Park et al. 2015; Kim et al. 2015; Park et al. 2017). Body shape models created from statistical analysis of these data have provided the first detailed information on child body shapes in seated postures (Park et al. 2017). Several of these body shape models are available online at http://humanshape.org/. Recently, the first ATD for which anthropometric specifications were developed using 3D body shape modeling was developed (Reed 2013).

In the current study, a manikin that represents the body size and shape of a typical U.S. child 24 months of age was developed. The external surfaces were developed from a statistical body shape model of young children and constructed using additive manufacturing techniques. An internal armature was designed to provide articulation in the neck and hips to enable positioning in a range of postures and seat conditions.

A study of child posture and belt fit was conducted to provide a database to which the manikin measures could be compared. The location of the belt with respect to the pelvis was recorded for a range of lap belt angles. The fit of a harness specifically designed for aviation seating was also measured. The belt fit data from children were compared to those obtained with the manikin to assess its validity.

METHODS — MANIKIN

In a recent study, laser scan data from 40 children ages 12 to 36 months were obtained in a range of postures (Kim et al. 2015). Scan data for a seated posture were fitted with a standardized template and a statistical analysis was conducted to predict body size and shape as a function of anthropometric variables. For the current study, the body shape of a seated toddler was parameterized by torso length (crown-rump length) and body weight. Figure 1 shows some example output from the model using values for an average 24-month-old child of 527 mm for crown-rump length and 12.3 kg for body weight (Snyder et al. 1977). Internal joint center locations were estimated from the palpated locations of surface body landmarks that are included in the body shape model (see Kim et al. 2015).
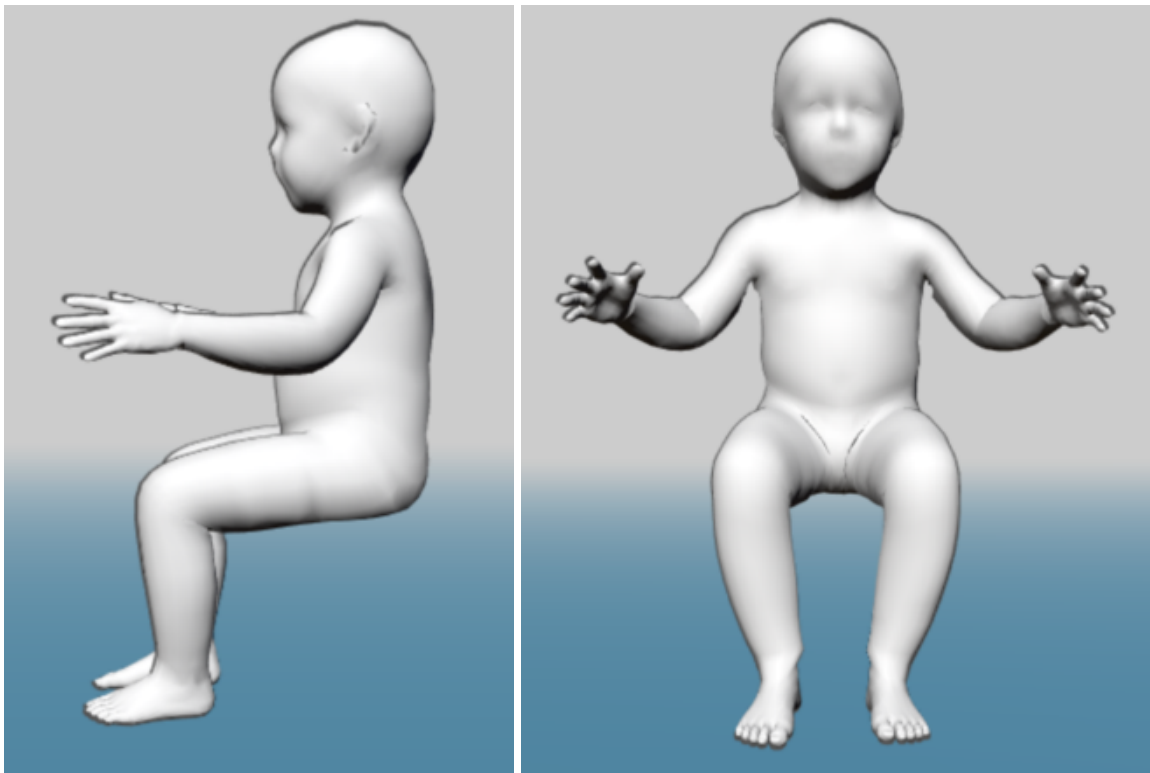

Figure 1. Output from statistical body shape model using torso length = 527 mm and body weight = 12.3 kg
(see Kim et al. and http://humanshape.org/)

A manikin design was developed using the external body shape and internal joint linkage. Figure 2 shows two views of the manikin design. A steel armature was created that provides the needed mass and includes hip joints and two neck joints. The neck joints are connected using a four-bar linkage that provides a single degree of freedom for head motion. Note that the neck motion is intended primarily to allow the back of the head to clear the seat surface across a range of postures.
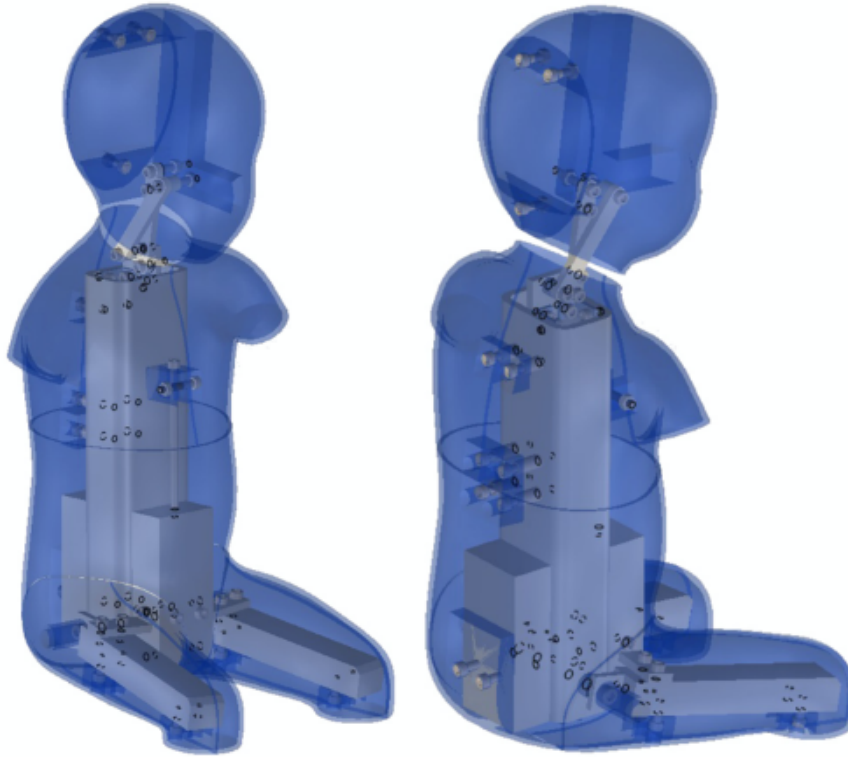
Figure 2. CAD model of manikin showing internal armature and surface shell segments.

The manikin surfaces were manufactured using acrylonitrile butadiene styrene (ABS) plastic with a 3D Dimension Elite printer. Following printing, the surfaces were smoothed by exposure to acetone vapor and then painted. The surface components are attached to the armature with conventional fasteners. Figure 2 shows the manikin in an aviation seat.
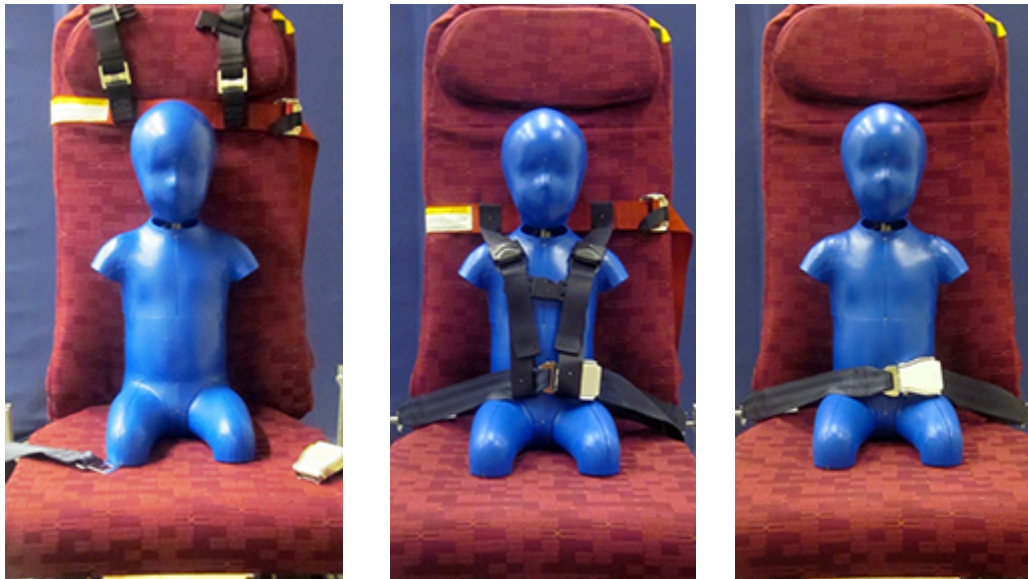

Figure 3. Manikin in an aviation seat.

METHODS — CHILD POSTURE AND BELT FIT

Overview of Approach

The protocol for this study was approved by an Institutional Review Board at the University of Michigan (approval HUM00118995). Body shapes and postures of children aged 12 to 47 months old were measured sitting in a range of seat and belt configurations on laboratory seat constructed from aviation seat components. Each child's body dimensions were characterized through manual measurements and whole-body surface measurement. A FARO Arm coordinate measurement machine was used to record the three-dimensional locations of body landmarks and the belt or harness system in each test condition. A hand-held three-dimensional surface digitizer (3D Systems Sense Scanner) was also used to record postures and contours. Full-body surface geometry was obtained in Vitus laser scanner in both standing and seated postures.

Test Fixture

Seat

Testing was carried out on a laboratory mockup of commercial aircraft seat. The surface geometry of the aircraft seat was measured using a handheld structured light scanner (Figure 4) and the angles of the seat back and cushion were measured with a SAE J826 H-point machine and associated procedures. The location of the seat H-point (SAE J836) and Seat Index Point (ISO 5353) were also measured (Figure 5). The cushions from the seat were removed and mounted on a frame built to recreate the geometry of the commercial seat. The 15.5-degree seat back angle and two-degree cushion angle (SAE J826) matched the aircraft seat when measured in its upright position. Figure 6 shows an overlay of the surface geometry of the mockup and the original aircraft seat.

Figure 4. Surface scans of an aircraft seat.

8

Figure 5. J826 H-point machine (left) and Seat Index Point Tool (right) used to characterize seat geometry.

Figure 6. Scan of aircraft seat (left), the mockup seat (middle), and overlaid (right).

Aircraft Restraint System

The purpose of the mockup was to create space around the seat for a fixture that allowed the lap belt anchorage to be adjusted over a wide range, which was not possible with the production seat. Using the FMVSS 210 definition, the lap belt angle in the aircraft seat was 54 degrees with respect to horizontal relative to the H-point (SAE J826) with a distance of 186 mm between the H-point and the anchor pivot point in XZ (side view) plane. Figures 7 and 8 show the lap belt fixture and the relative location of the anchorage to the H-point. The lap belt from the aircraft seat was used in this study without modification except for changes in the anchorage locations. The lap belt width was 48 mm, although the area near the latchplate is slightly narrower due to the stitching used to attach the latchplate.
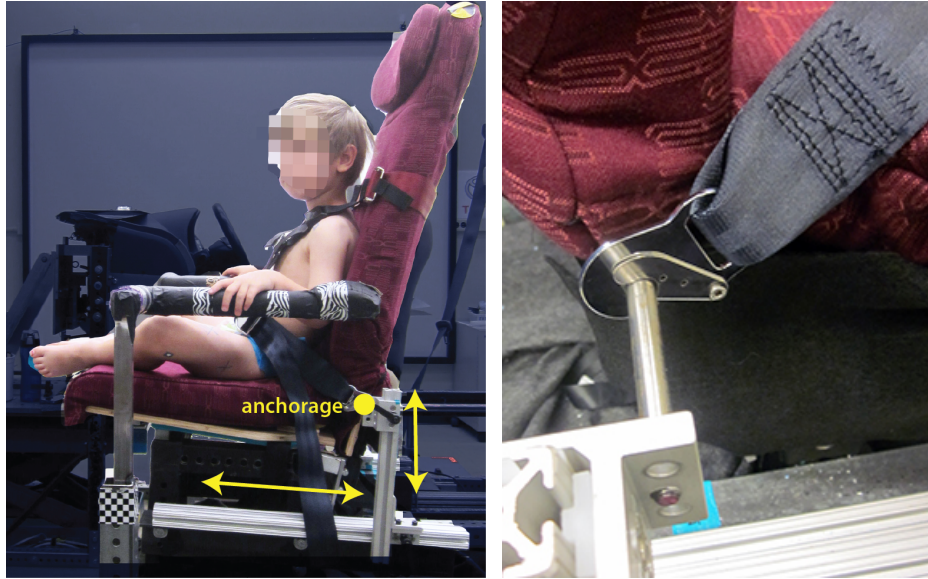
Figure 7. The anchorages for the lap belt were mounted on a track that moved fore-aft and up-down. The lap belt latch clipped to a bar that brought the anchorage point inboard to the location measured on the aircraft seat.
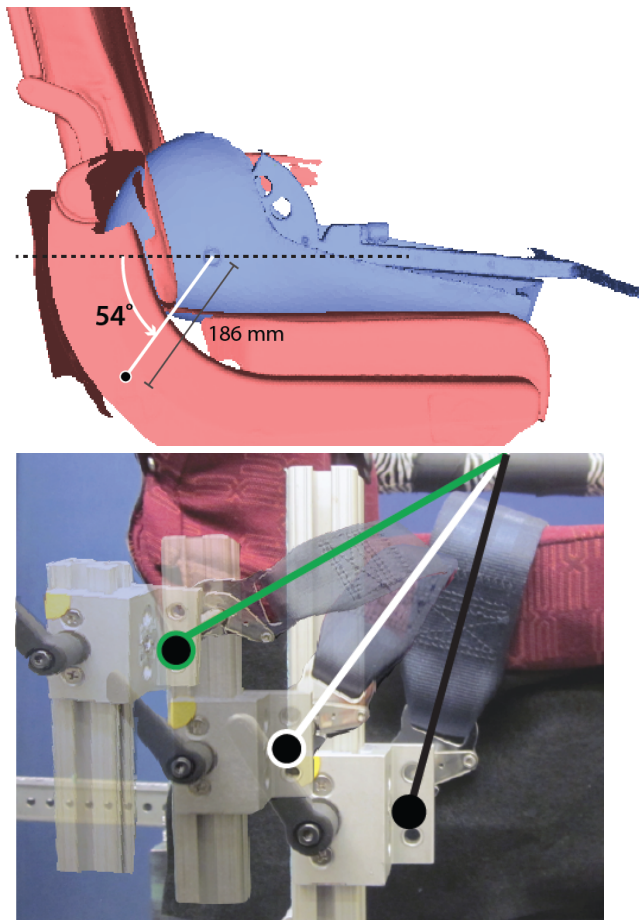

Figure 8. Lap belt anchorage location relative to H-point machine in the aircraft seat (top) and the range of anchorage angles in the mockup (bottom).

The AmSafe Child Aviation Restraint System (CARES), shown in Figure 9, is the only harness-type aviation child safety device (ACSD) certified by the Federal Aviation Administration as an alternative to a car seat (Part No. 4082, 14 CFR § 21.8(d), or TSO-C100b, or a later version). According to the FAA certification for CARES, the FAA states "The system is for use by children between 22 and 44 lb. (~10-20 kg) in weight, less than 40 inches (~101 cm) tall and who are capable of sitting upright alone in a forward-facing position." A CARES was purchased online and used without modification according to the CARES instructions.

Figure 9. Aircraft seat as manufactured on aluminum frame (left), aircraft seat cushions mounted on laboratory frame with lap belt (center) and lap belt plus CARES harness (right).

Test Conditions

The test conditions (Table 1) included three lap belt angles (Figure 8) that spanned the range of angles allowed in FMVSS 210 from a steep angle of 75 degrees relative to horizontal to a flat belt angle of 30 degrees. The 54-degree angle of the aircraft seat fell approximately midway between these extremes. The anchorage was moved in an arc around the H-point, therefore the side-view distance between the anchorage and the H-point remained constant across conditions. The CARES harness was tested with the lap belt at each of these angles.

Table 1. Test Conditions

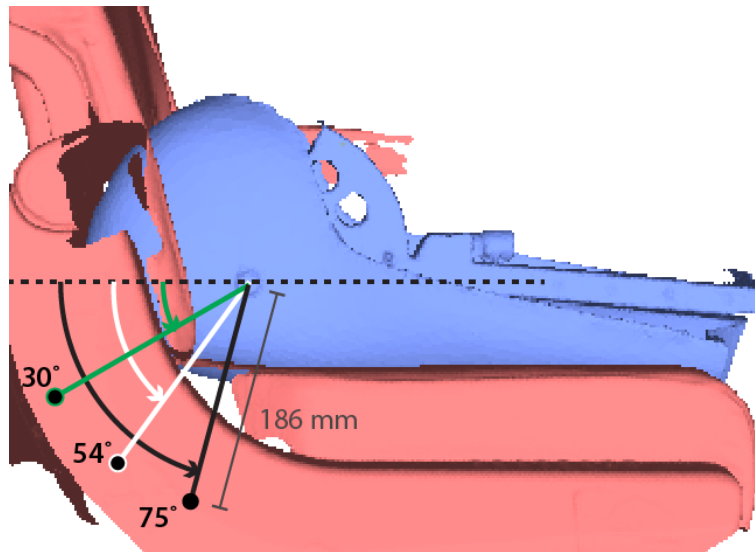|	Condition Name	Lap Belt Angle w.r.t. horizontal (degrees)	Restraint Type	Posture
1	CS_B_30d	30		
2	CS_B_54d	54	2-pt lap belt	
3	CS_B_75d	75		Child Selected
4	CS_H_30d	30		
5	CS_H_54d	54	2-pt lap belt + CARES harness	
6	CS_H_75d	75		
7	AS_B_30d	30		
8	AS_B_54d	54	2-pt lap belt	
9	AS_B_75d	75		Adult Selected
10	AS_H_30d	30		
11	AS_H_54d	54	2-pt lap belt + CARES harness	
12	AS_H_75d	75		

Figure 10. Anchorage locations included in test matrix

In an attempt to capture a range of child postures, the participants were measured in "child-selected" and "adult-selected" postures. The baseline requirements for both postures were that the child's buttock area was on the seat cushion (not kneeling, for example) and some part of the child's back, neck or head was against the seat back. For all conditions, the parents stayed with their children and helped distract them with toys or electronic devices. The lap belt and harness were placed on the child by the parent with the investigators helping to ensure a snug fit.

For the child-selected posture, the investigator asked the parent to place the child in the seat and was told to *"allow your child to sit comfortably, as though they are going to have to sit there for quite a while."* There were no posture requirements other than the baseline stated above. The pelvis was allowed to be any child-selected distance from the seat back that still allowed the restraint system to be snug against the child. For the adult-selected posture, which always was introduced after the child-selected conditions were completed, the investigator directed the parent to place the child all the way back in the seat, so that the child's back of the buttock area touched the seat back. The investigator also made sure the child was laterally centered on the seat and not leaning to the side.

Protocol

Thirty-eight children (nineteen boys and nineteen girls) aged 12 to 47 months of age were recruited for this study through their caregivers. All test procedures and recruiting materials were approved by the University of Michigan Institutional Review Board (HUM00118995). After providing written informed consent, parents changed the children changed into either a swimsuit or a pull-up diaper. The child was then measured with standard anthropometry, in a specially build laboratory *hardseat*, in the aircraft seat mockup, and in a 3D surface scanner. The order of these steps was sometimes changed to accommodate the behavior of the child.

The investigator used a FARO Arm coordinate digitizer to record the three-dimensional locations of landmarks on the participant's body and on the mockup, seat, and belt. Table 2 lists all of these points. Figures 11-13 shows the locations of the points recorded. The child was measured three times in each condition. The first set of measurements was a quick subset of the landmarks to ensure usable posture data from all children, including the most mobile. The second set of measurements was the lap belt and harness belt points and streams plus the skeletal landmarks used in assessing belt fit. The purpose was to ensure that the restraint points and points on the underlying bones were recorded as closely as possible together in time in case the child had difficulty sitting still. The final set of measurements was a complete set of landmark points characterizing posture from head to toe. The parent or the investigator helped the child stay still during this set. In addition, a stream of points with approximately 5-mm spacing was recorded along the edges of the lap and harness portions of the belt between the anchorages (Figure 14).

Table 2. Points Recorded on Participant, Restraints, and Mockup

First: Quick Posture List
  C7 (Cervicale)
  Tragion Rt
  Suprasternale
  Substernale
  ASIS Rt
  Suprapatella Rt
  Lateral Femoral Epicondyle Rt
  Lateral Malleolus Rt

Second: Seat, Restraint System, and Belt Fit
Seat:
  4 seat reference points
  Lap belt anchorage point Lt and Rt
Lap Belt:
  Lap belt top and bottom at Lt and Rt ASIS and
  midline
  Buckle center
  Stream of points along the top edge of the belt
Harness:
  3 reference points Lt and Rt
  Harness inboard edge at suprasternale height Lt
  and Rt
  Harness inboard edge on clavicle Lt and Rt
  Harness outboard edge on clavicle Lt and Rt
  Center harness clip
  Streams of points along the inboard edges of the
  harness
Child
  C7 (Cevicale)
  Suprasternale
  Substernale
  ASIS Rt and Lt
  Suprapatella Rt and Left

Third: Complete Posture List
 C7 (Cervicale)
 Back Of Head (Max Rearward)
 Top Of Head (Max Height)
 Tragion Rt
 Ectoorbitale Rt
 Infraorbitale at Pupil Center Rt
 Glabella
 Suprasternale
 Substernale
 Medial Clavicle Rt
 Lateral Clavicle Rt
 Anterior of Acromion Lt and Rt
 Lateral Humeral Epicondyle Rt
 Ulnar Styloid Process, Lateral Rt
 ASIS Lt and Rt
 Suprapatella Lt and Rt
 Infrapatella Lt and Rt
 Lateral Femoral Epicondyle Lt and Rt
 Medal Femoral Epicondyle Lt and Rt
 Toe (longest point) Lt and Rt
 Ball of Foot Lateral Lt and Rt
 Ball of Foot Medial Lt and Rt
 Heel (Bottom edge of sole at midline) Lt and Rt
 Lateral Malleolus Lt and Rt
 Medial Malleolus Lt and Rt

Figure 11. Investigator digitizing points on restraint system
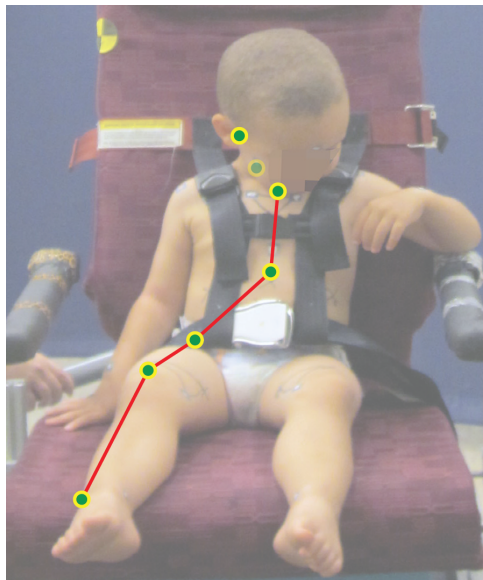

Figure 12. The subset of points digitized to get a quick "snapshot" of the child's posture in case the child had difficulty sitting still
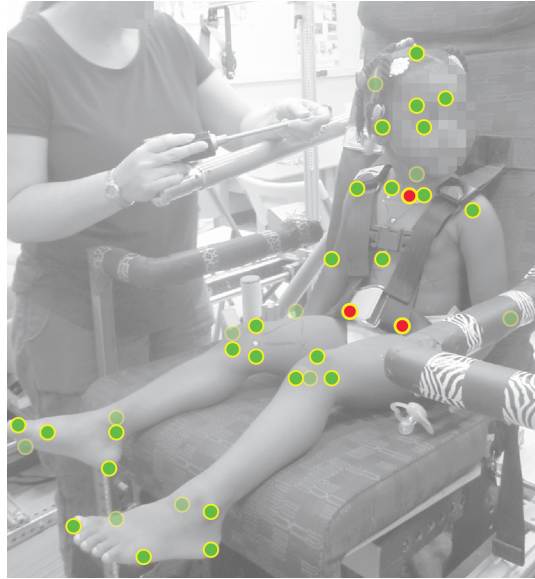
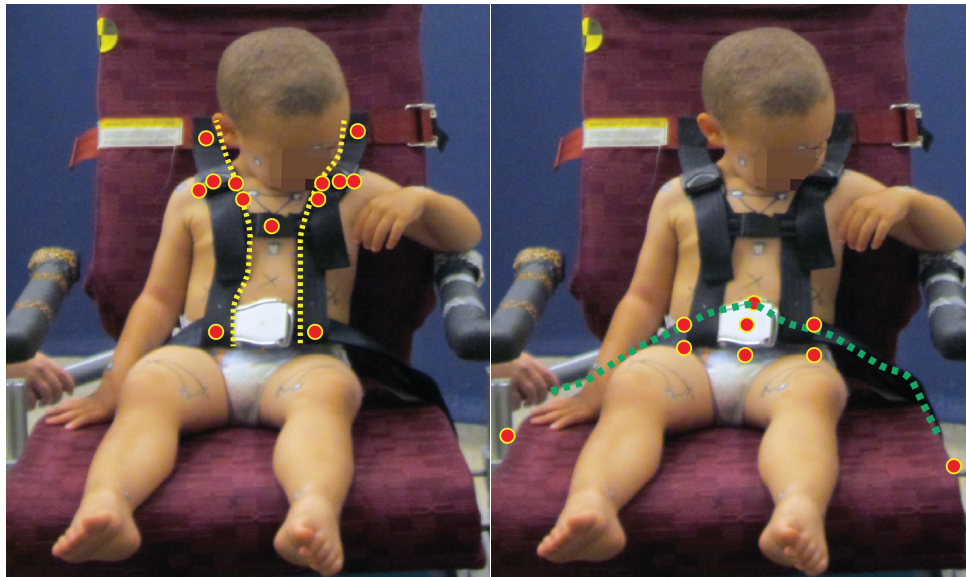Figure 13. Longer list of points digitized on child to characterize posture

Figure 14. Points and streams of point recorded on the harness and lap belt; the lap belt was also recorded in harness trials (not showing skeletal landmarks recorded at same time)

Hardseat

Body landmark locations were recorded in the laboratory hardseat shown in Figure 15. The hardseat allows access to posterior spine and pelvis landmarks that are inaccessible in the aircraft seat. The hardseat has a 15˚ back angle and 7˚ "cushion" (pan) angle designed to produce postures similar to the "adult-selected" postures in the aircraft seat. Table 3 lists the landmarks

recorded in the hardseat. Figure 16 shows a participant being measured in the seat. A cushion was placed under the knees of the children to help them maintain the posture. A harness system from a child restraint system was used to safety secure the child in the hardseat.

The landmark set and measurement methods were derived from those used in previous studies of automotive posture for both adults and children (Reed et al. 1999, Reed et al. 2005). Each of anatomical linkages in Table 3 was measured separately to reduce the time required to complete each set, as the children often had difficulty holding a posture. By design, there was redundancy in digitized anatomical points between the individual linkage segments. The intention was to ensure that points from a linkage could be used to align the anatomical location recorded in a different linkage.
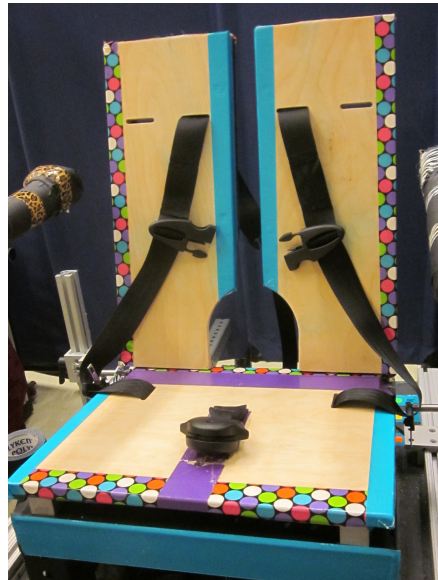

Figure 15. Hardseat with opening in seat back to allow access to spline and pelvis and a child restraint harness to help keep the child in position

Figure 16. Child sitting in the hardseat (left) and an investigator digitizing the child's spine and pelvis through the opening in the back of the seat (right)

Table 3. Hardseat Landmarks and Scanning Markers

Back of Head	Substernale	C7
Top Of Head (Vertex)	**Substernale Marker**	**C7 Marker**
Tragion Lt and Rt	Chest Triad Markers (3)	T4
Ectoorbitale Lt and Rt	**Torso Marker Lt and Rt**	**T4 Marker**
Infraorbitale at Pupil Center Lt and Rt	**Torso Mid Top Marker**	T8
Glabella	**Torso Mid Bot Marker**	**T8 Marker**
Head Center Marker	**Hip Marker Lt and Rt**	T12
Head Marker Lt and Rt	**Upper Leg Lateral Marker Lt and Rt**	**T12 Marker**
Medial Clavicle Lt and Rt	**Upper Leg Medial Marker Lt and Rt**	L1
Lateral Clavicle Lt and Rt	**Upper Leg Anterior Marker Lt and Rt**	**L1 Marker**
Acromion Lt and Rt (Anterior)	Lateral Femoral Epicondyle Lt and Rt	L2
Acromion Marker Lt and Rt	**Lateral Femoral Epicondyle Marker Lt and Rt**	**L2 Marker**
Humeral Epicondyle Lateral Lt and Rt	Medial Femoral Epicondyle Lt and Rt	L3
Lateral Elbow Marker Lt and Rt	**Medial Femoral Epicondyle Marker Lt and Rt**	**L3 Marker**
Humeral Epicondyle Medial Lt and Rt	Suprapatella Lt and Rt	L4
Medial Elbow Marker Lt and Rt	Infrapatella Lt and Rt	**L4 Marker**
Ulnar Styloid Process Lt and Rt	Heel Lt and Rt	L5
Radial Styloid Process Lt and Rt	Lateral Ankle Lt and Rt	**L5 Marker**
Wrist Mid Top Marker Lt and Rt	**Lateral Ankle Marker Lt and Rt**	ASIS Lt and Rt
Wrist Mid Bottom Marker Lt and Rt	Ball of Foot Lateral Lt and Rt	PSIS Lt and Rt
Lateral Hand Lt and Rt	Toe (Longest Tibiale) Lt and Rt	
Medial Hand Lt and Rt	Ball of Foot Medial Lt and Rt	
Suprasternale	Medial Ankle Lt and Rt	
Suprasternale Marker	**Medial Ankle Rt Marker**	

Anthropometrics

Standard Anthropometry

Anthropometric data were gathered from each child to characterize the overall body size and shape. The standard anthropometry measures listed in Table 4 were obtained using manual measurements. Procedures for obtaining manual measures of child anthropometry are outlined in Snyder et al. (1977). Standard anthropometry techniques were detailed by Snyder to measure children less than 2 years of age in a supine posture and children over 2 years in a standing posture. During the study, some of the measurements were taken in standing/seated and supine to allow comparisons with values in the literature. Definitions of the standard anthropometric measures are presented in Appendix B. Anthropometric measures obtained from multiple postures provide preliminary data on how these anthropometric measures vary with posture. If child was not cooperative, a subset of measures was taken. An example of measuring knee height and erect sitting height in seated and supine postures is illustrated in Figure 17.

Figure 17. Example of knee height and erect sitting height measurements in both seated and supine postures.

Table 4. Anthropometric measures

Measurement	Standing	Sitting	Supine
Weight	X*	Alt.	
Stature	X		X
Bideltoid Breadth	X	Alt.	X
Biacromial Breadth	X	Alt.	
Chest Breadth	X	Alt.	Alt.
Waist Breadth at Omphalion Height	X	X	
Waist Depth at Omphalion Height	X		
Shoulder-Elbow Length	X	Alt.	Alt.
Elbow-Fingertip Length	X	Alt.	Alt.
Bispinous Breadth (Bi-ASIS)	X	Alt.	Alt.
Pelvis Breadth	X		Alt.
Pelvis Depth (ASIS to PSIS)	X		Alt.
Chest Depth (On Spine)	X	Alt.	Alt.
Maximum Hip Breadth		X	X
Buttock-Knee Length		X	X
Buttock-Popliteal Length		X	X
Erect Sitting Height		X	X
Seated Eye Height		X	X
Seated Shoulder Height		X	X
Knee Height		X	X
Tragion to Top of Head	Alt.	X	Alt.
Head Breadth	Alt.	X	Alt.
Head Length	Alt.	X	Alt.
Head Circumference	X	Alt.	
Chest Circumference at Axilla	X	Alt.	
Waist Circumference at Omphalion	X		
Maximum Hip Circumference	X		
Thigh Circumference at Gluteal Fold	X		
Maximum Calf Circumference	X	Alt.	
Ankle Circumference above Malleolus	X	Alt.	
Mid Upper Arm Circumference	X	Alt.	
Maximum Forearm Circumference	X	Alt.	
Date of Birth			
Gender			

*X=preferred posture, Alt.=alternate posture

Whole-Body Scanning

Body shape and surface contours were recorded using a Vitronic Vitus XXL full-body laser scanner and Scanworx software (HumanSolutions). The VITUS XXL records hundreds of thousands of data points on the surface of the body in about 12 seconds by sweeping four red, eye-safe lasers vertically. The two cameras on each of the four scanning heads pick up the laser light contour projected on the participant and translate the images into accurate three-dimensional data. Figure 18 shows a participant being scanned and Figure 19 shows sample data. Appendix B provides additional details on the scan postures and procedures.
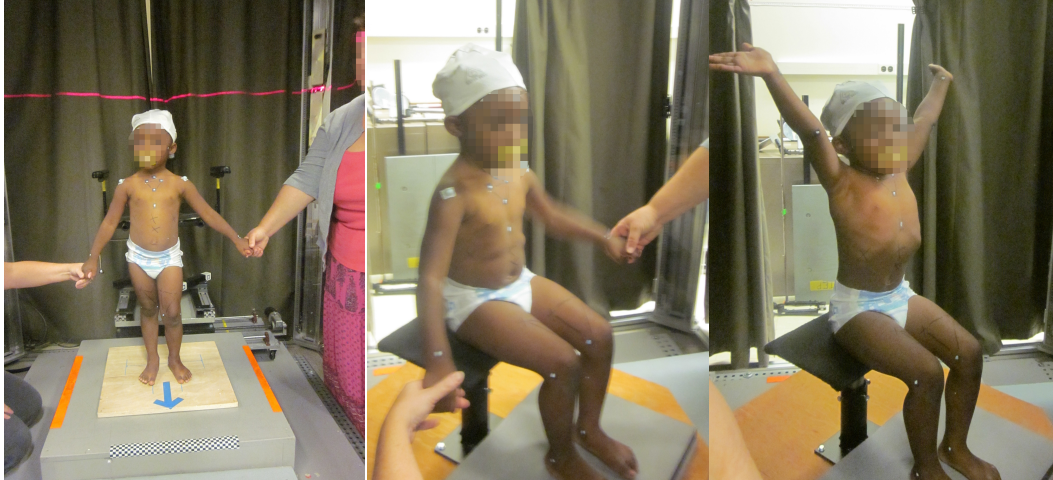
Figure 18. Participant in full-body laser scanner

Figure 19. Sitting and standing postures in the full-body scanner

The locations of landmarks on the participants were recorded via skin targets stamped on the skin. Body landmarks were marked on the skin using a pattern of water soluble, non-toxic, square ink stamp into which was placed a high contrast white paint dot (Figures 20 and 21). Appendix A describes the scanning process and postures in more detail.
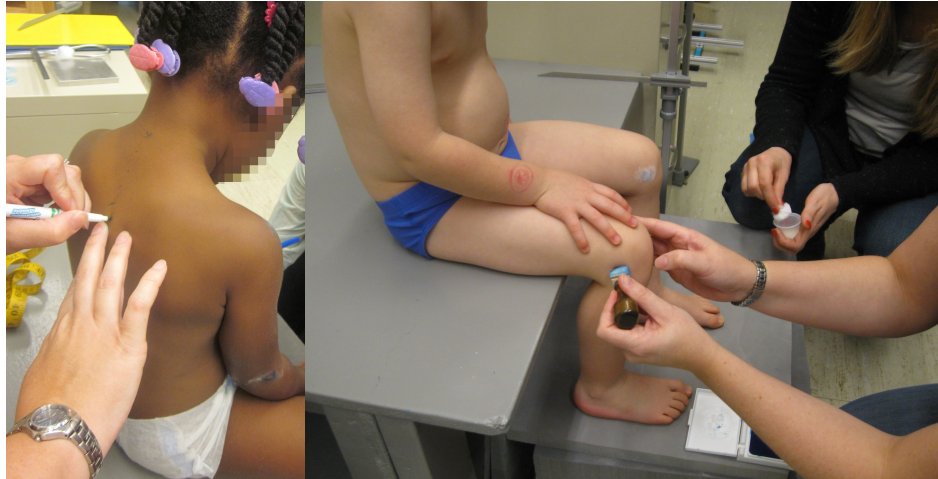
Figure 20. Marking landmarks (left) and stamping (right) skeletal landmarks on child participants
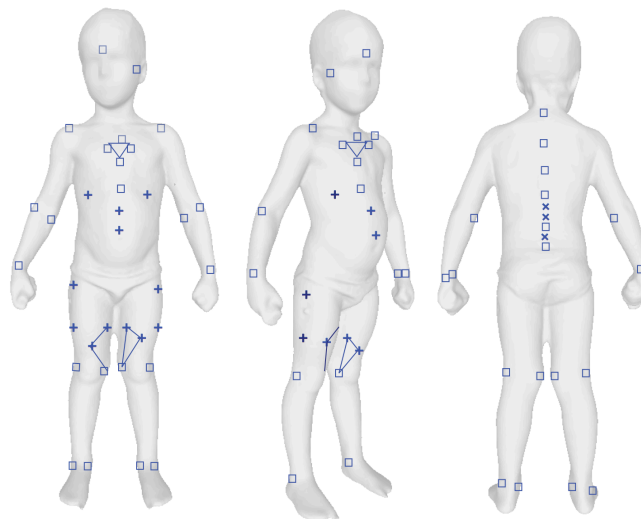
Figure 21. Targets stamped on participant to track skeletal landmarks and track changes in torso shape across postures.

Table 5. Scanning Marker List

Point Name	Body Part	Additional Description
HeadCenter_M	Head	Marker on forehead
HeadLt_M	Head	Marker near tragion where face doesn't move
HeadRt_M	Head	Marker near tragion where face doesn't move
AcromionLt_H	Torso	Center point on acromion hemisphere
AcromionRt_H	Torso	Center point on acromion hemisphere
ElbowMedLt_M	Arm	Medial epicondyle (mark with elbow bent 45˚) (inside of elbow)
ElbowMedRt_M	Arm	Medial humeral epicondyle (mark with elbow bent 45˚)
ElbowLatLt_M	Arm	Lateral epicondyle (mark with elbow bent 45˚) (outside of elbow)
ElbowLatRt_M	Arm	Lateral humeral epicondyle (mark with elbow bent 45˚)
WristMidTopLt_M	Arm	On the back of the wrist slightly proximal to the cross section plane of the ulnar styloid.
WristMidTopRt_M	Arm	On the back of the wrist slightly proximal to the cross section plane of the ulnar styloid.
WristMidBotLt_M	Arm	On the palm side of the wrist opposite the wrist mid marker
WristMidBotRt_M	Arm	On the palm side of the wrist opposite the wrist mid marker
SpineC07_M	Torso	Spinous process of the 7th cervical vertebra (cervicale)
SpineT04_M	Torso	Spinous process of 4th thoracic vertebra
SpineT08_M	Torso	Spinous process of 8th thoracic vertebra
SpineT12_M	Torso	Spinous process of 12th thoracic vertebra
SpineL01_X	Torso	Spinous process of 1st lumbar vertebra
SpineL02_X	Torso	Spinous process of 2nd lumbar vertebra
SpineL03_M	Torso	Spinous process of 3rd lumbar vertebra
SpineL04_X	Torso	Spinous process of 4th lumbar vertebra
SpineL05_M	Torso	Spinous process of 5th lumbar vertebra
SternSup_M	Torso	Marker on suprasternale
SternSup22Y18ZLt_M	Torso	Marker 18 mm down and 22 to left of suprasternale
SternSup22Y18ZRt_M	Torso	Marker 18 mm down and 22 to right of suprasternale
SternSup60ZCt_M	Torso	Marker 60 mm down from suprasternale
SternSub_M	Torso	Marker on substernale
TorsoMidUpperCt_X	Torso	X below the bottom of the sternum
TorsoMidLowerCt_X	Torso	X above the omphalion and below TorsoMidUpperCt_X
TorsoLt_X	Torso	X on torso outside of harness
TorsoRt_X	Torso	X on torso outside of harness
HipLt_X	Leg	Lateral most point at thigh junction with hip
HipRt_X	Leg	Lateral most point at thigh junction with hip
UpperLegLatLt_X	Leg	Lateral most point at mid thigh height
UpperLegLatRt_X	Leg	Lateral most point at mid thigh height
UpperLegMedLt_X	Leg	Medial most point at mid thigh height
UpperLegMedRt_X	Leg	Medial most point at mid thigh height
KneeFemMedLt_M	Leg	Femoral epicondyle, medial
KneeFemMedRt_M	Leg	Femoral epicondyle, medial
KneeFemLatLt_M	Leg	Femoral epicondyle, lateral
KneeFemLatRt_M	Leg	Femoral epicondyle, lateral
UpperLegAntLt_X	Leg	Center of thigh between mid thigh height and knee
UpperLegAntRt_X	Leg	Center of thigh between mid thigh height and knee
AnkleLatLt_M	Leg	Malleolus, lateral
AnkleLatRt_M	Leg	Malleolus, lateral
AnkleMedLt_M	Leg	Malleolus, medial
AnkleMedRt_M	Leg	Malleolus, medial

Belt-Fit Calculations

Lap belt fit was quantified using procedures similar to those used previously for both adults and children (Reed et al. 2008a). The location of the upper edge of the lap belt was digitized at the lateral location (relative to the pelvis) of the anterior-superior iliac spine (ASIS) landmark (Figure 22). The fore-aft and vertical (X and Z) location of the belt with respect to the ASIS was analyzed to compare belt fit across conditions. Ideal belt fit would be indicated by the upper edge of the belt lying close to the ASIS. Belt positions higher than the ASIS create an increased risk of abdomen loading, and belt positions further forward may indicate slack in the belt and would allow greater forward excursions.
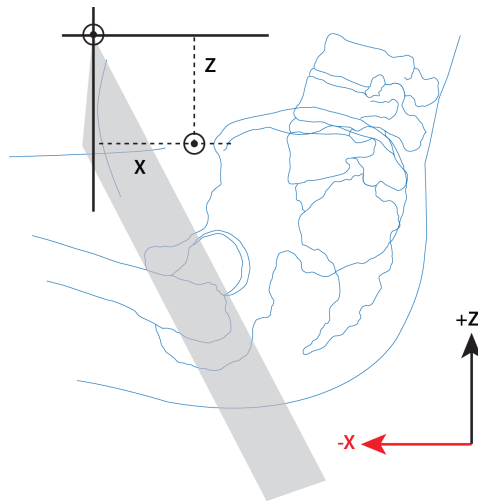
Figure 22. Dependent measures for lap belt fit. The upper/rearward edge of the lap portion of the belt is measured at the lateral position of the right and left the predicted ASIS location. The fore-aft (X) coordinate is positive rearward of the ASIS and the vertical coordinate is positive above the ASIS landmark.

Harness fit was quantified by measuring the inner edge of the right harness strap with respect to the child centerline at the height of the suprasternale landmark. As described in the results section, harness fit was largely determined by the geometry of the chest clip and hence did not vary substantially across child body size.
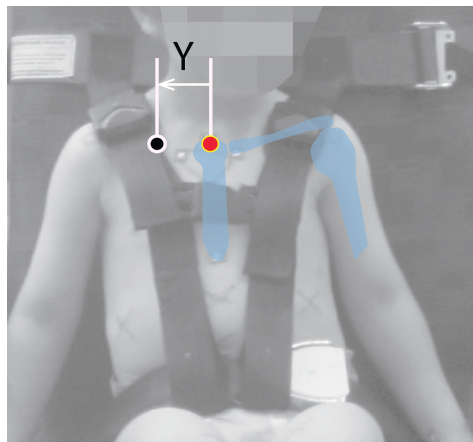

Figure 23. Harness point at suprasternale height

Other Data Collected

While the child was in the test seat, three-dimensional scan data were gathered using the handheld Sense scanner. Figure 24 shows an example of data from the scanner. Time-lapse images were also obtained in the laboratory to provide a record of the range of child postures (Figure 25). These data were not analyzed for the current report but are available for future studies.

.

Figure 24. Participants were also scanned while in aircraft seat using a Sense hand-held scanner.

Figure 25. Time-lapse pictures showing range of child postures.

Manikin Belt Fit Measurement

A procedure was developed to repeatably seat the manikin, apply the restraint, and measure the resulting posture and belt fit. Figures 62 and 63 shows some of the steps and example installations. The full procedure is listed in Appendix C. For the current analysis, the belt fit is assessed using procedures analogous to those used for children: the location of the upper edge of the belt is compared with the surface ASIS location on the right side (away from the buckle).
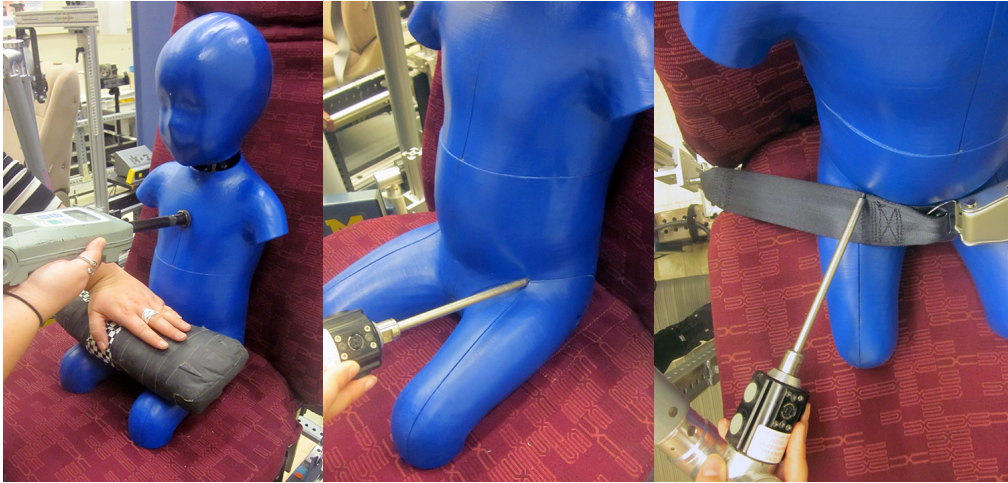
Figure 62. Installing the manikin (left), digitizing its location (middle), and then digitizing belt fit (right)

Figure 27. Photos of the manikin with a harness and lap belt.

RESULTS

Standard Anthropometric Measures

Table 6 summarizes selected standard anthropometric measures for the study population. On average the children were 31 months old at testing with a supine torso length of 573 mm and a mass of 13.5 kg. These compare favorably with the analogous reference dimensions for the manikin of 527 mm and 12.3 kg, although on average the children were older and larger. Note that the analysis methods take into account body size when such effects are significant and consequently do not require that the population sample mean match the manikin reference dimensions. Figure 28 shows plots of stature, body weight, torso length, and age.

Table 6. Summary of Selected Anthropometric Measures

Measure	Mean	SD	Min	Max
Stature (mm)	901.2	88.6	715.0	1063.0
Age (months)	30.8	10.4	12.0	47.0
Weight (kg)	13.5	2.4	8.5	19.3
BMI (kg/m^2)	16.6	1.4	13.9	19.8
Torso Length Supine (mm)	572.5	41.9	496.0	656.0
Sitting Height (mm)	532.0	42.2	455.0	603.0
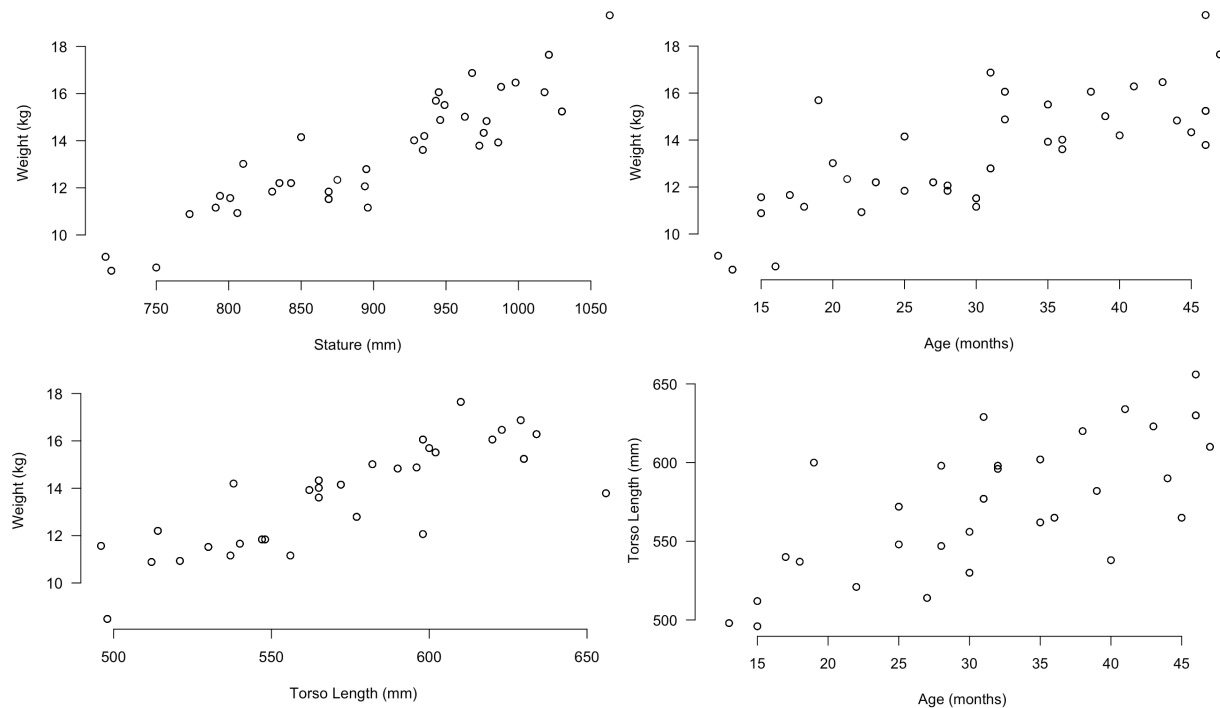
Figure 28. Plots of anthropometric variables for study population.

27

Lap Belt Fit

The horizontal and vertical placement of the lap belt was assessed across lap belt angles and posture category (child-selected or adult-selected). Based on the behavior of the children and their care-givers, some postures that were nominally child-selected were reclassified as adult-selected. Table 7 lists the number of postures in each category for the lap belt trials (three belt angles).

Table 7. Classification of Lap Belt Trials

Posture (Number of Trials)	Lap Belt Angle (deg)		
	30°	54°	75°
Adult-Selected	23	25	24
Child-Selected	21	19	20

Lap belt fit did not differ markedly between child- and adult-selected postures. Figure 29 compares the X and Z lap belt scores in child- and adult-selected postures across belt angles for lap-belt-only trials. No significant differences were observed, so both categories were pooled for subsequent analysis of belt angle effects. Figure 30 shows that the pooled X and Z scores are uncorrelated.
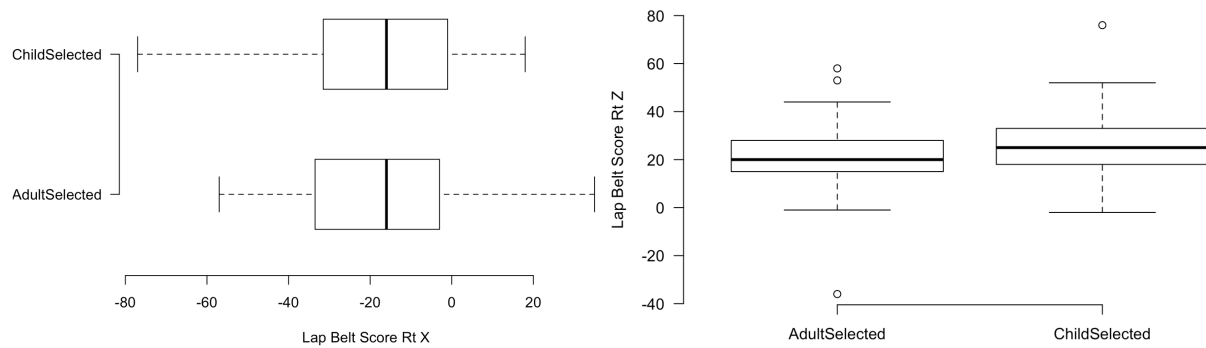
Figure 29. Box plots comparing lap belt fit (mm) in child- and adult-selected postures across belt angles.
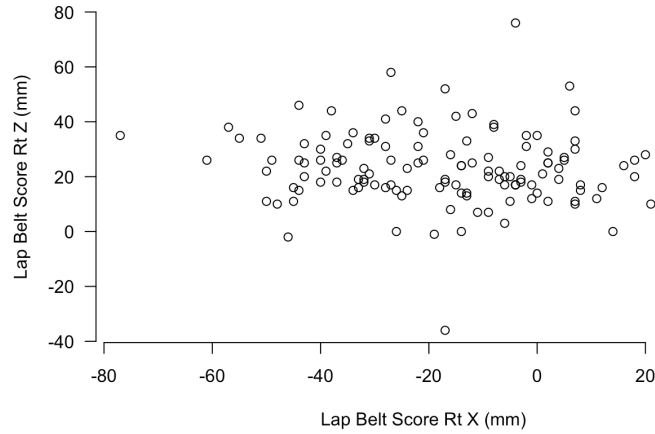
28

Figure 30. Crossplot of lap belt X and Z scores for pooled data from both adult- and child-selected postures.

Figure 31 shows the effect of belt angle on the lap belt fit. Steeper belt angles (54 or 75 degrees) were associated with belt positions that were further forward and lower relative to the ASIS landmark. An ANOVA found no significant difference in belt fit between the 30- and 54-deg conditions for X and 54- and 75-deg conditions for Z.
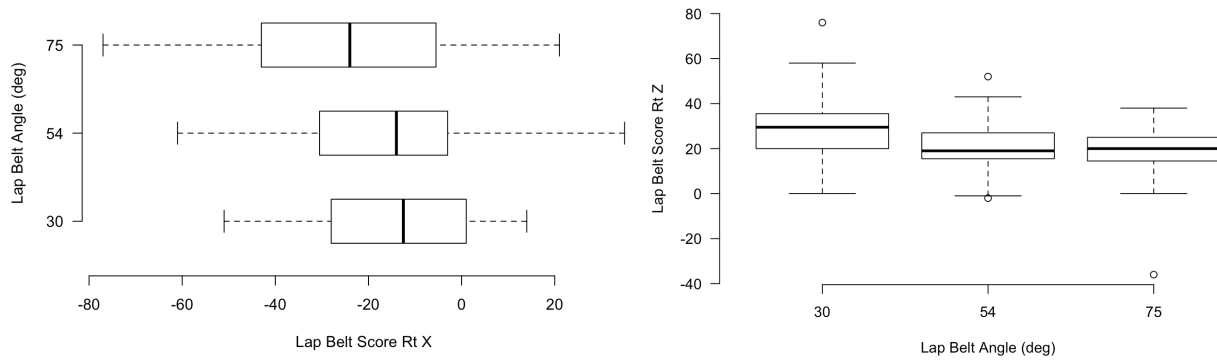

Figure 31. Box plots comparing lap belt fit (mm) across belt angles for pooled data from both adult- and child-selected postures.

Figure 32 shows the lap belt scores as a function of anthropometric variables. Larger children, associated with larger stature, body mass, and torso length, experienced lap belt positions more rearward and lower (closer to the pelvis) on average. However, variability at any particular body size was large.
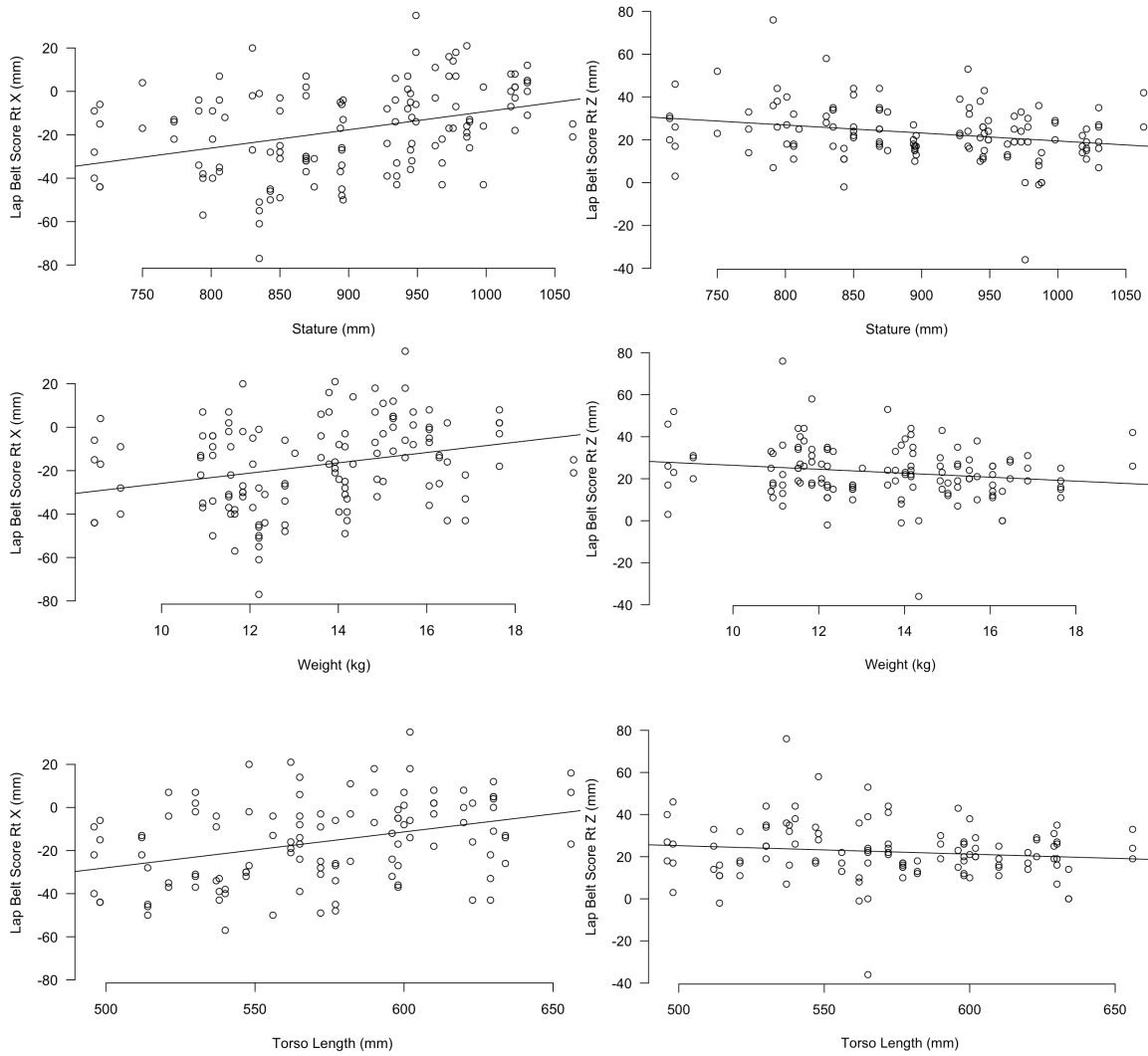
Figure 32. Lap belt scores as a function of anthropometric variables across three belt angles. Torso length is supine crown-rump length.

Linear regression models predicting belt scores from anthropometric variables showed significant ($p<0.05$) but small effects of both lap belt angle and body dimensions (equations 1 and 2). Interactions were not significant, nor were second-order effects of lap belt angle. As shown in equations 1 and 2, the adjusted R^2 value indicates than less than 15% of variance was accounted for by the predictors.

$$LapBeltScoreRtX = -37.8 - 0.218\ LapBeltAngle + 2.35\ Weight, R^2_{adj} = 0.10, RMSE = 19.3\ mm \qquad [1]$$

$$LapBeltScoreRtZ = 49.1 - 0.244\ LapBeltAngle - 0.97\ Weight, R^2_{adj} = 0.13, RMSE = 0.14\ mm \qquad [2]$$

for LapBeltAngle in degrees and body weight in kg.

Harness Fit

The CARES harness is attached to the lap belt as well as the seat. The harness position with respect to the midline of the body was measured on the child's left and right sides at the height of the suprasternale landmark. The left and right harness scores were slightly correlated (Figure 33), reflecting differences due to the child leaning to one side. Harness width, i.e., the distance between the inside edges of the two harness straps at the height of the suprasternale landmark, was not significantly related to body size (Figure 34). Note these values are affected by movement of the child between point measurements. Harness fit was not significantly related to body size and was not influenced by lap belt angle (Figure 35). The harness shifted the lap belt an average of 13 mm rearward and 26 mm higher relative to the pelvis (Figure 36).
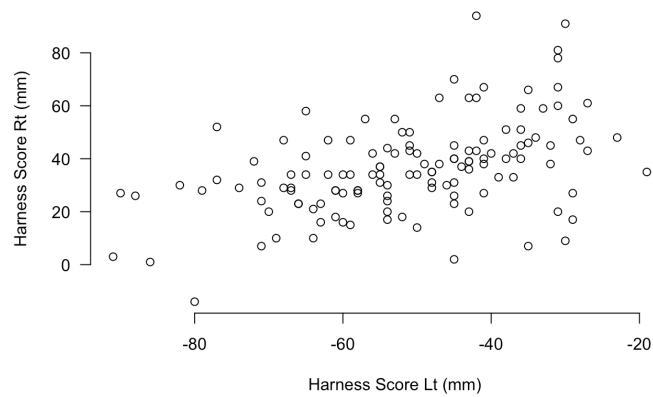
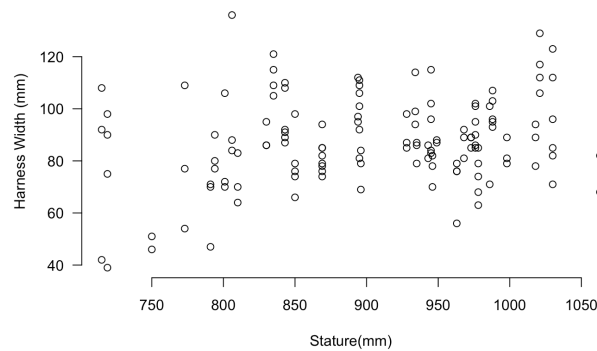Figure 33. Crossplot of harness scores on left and right side.

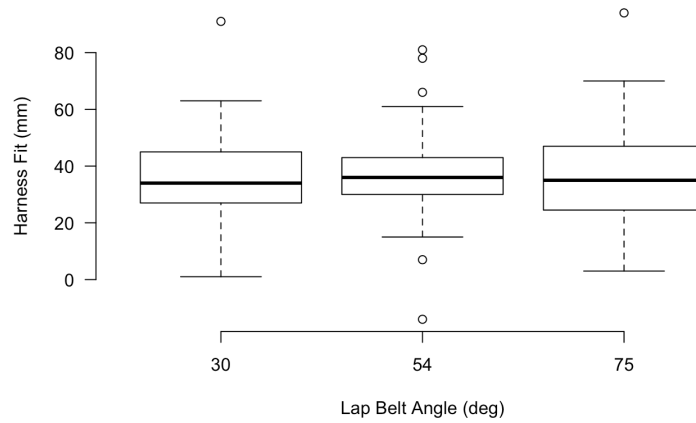Figure 34. Measured lateral distance between harness straps.
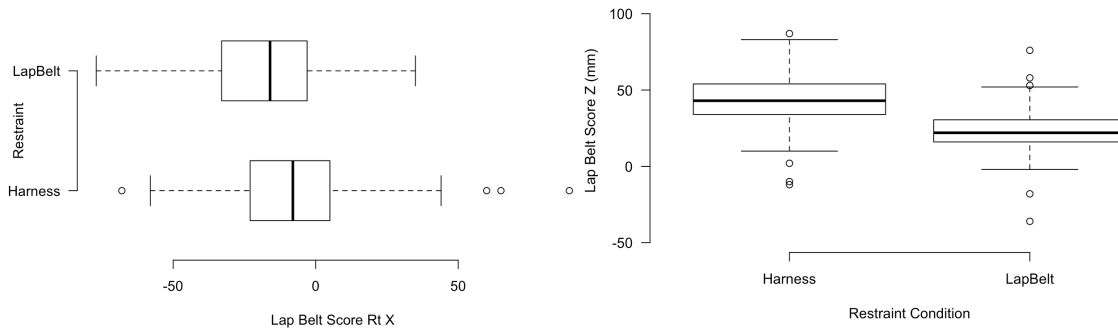
Figure 35. Harness fit and lap belt angle.

Figure 36. Effect of harness on lap belt score.

Child-Selected Postures

Children chose a wide range of postures, even within the constraints imposed by the test conditions. Particular variability was observed among the lower-extremity postures, as shown in Figure 37. An examination of several posture measures, including head height and fore-aft pelvis location, did not find significant differences between adult- and child-selected postures.

Relaxed legs (P021 CSB75)

Legs crossed (P004 CSB54)

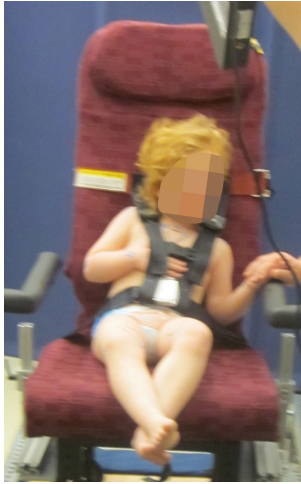Frog legs (P005 CSB54)

Feet flat against each other
(P001 CSB54)

Right leg bent, left leg relaxed
(P009 CSH30)

Left leg bent, right leg relaxed
(P003 CSH54)

Figure 37a. Examples of child postures.

Feet crossed (P003 CSH75)	Knees up (P005 CSH75)	Knees up (P012 CSH75)

Torso centered (P023 CSB30)	Torso left (P010 CSB30)	Torso right (P019 CSB54)	Torso right (P019 CSH75)

Figure 37b. Examples of child postures.

Belt Fit on Manikin

Table 8 summarizes the belt fit measures obtained using the manikin and the procedures described in Appendix C. Measurements were made in each condition by 3 investigators. The lap belt location with respect to the ASIS surface landmark is expressed with respect to the X and Z axes, as with the children. On average, the belt was 11 mm lower and 10 mm more rearward (i.e., closer) to the pelvis with the manikin than the children. Both the X and Z values on the manikin were affected by lap belt angle, following the same directional trends observed with the children, but the differences between manikin and child belt fit were larger at the 75-degree belt angle. Due to the mean difference in belt location on the manikin and children, moving from the 54° belt angle to 75° tended to move the belt lower on the manikin and further forward on the children. Note, however, that these trends are small relative to the within-condition variance for

children. For example, the range of mean lap belt Z across belt conditions for children is approximately the same as the within-condition standard deviation.

Table 8. Lap Belt Fit on the Manikin* and Children in Lap Belt Trials

| | Lap Belt X | | | | | Lap Belt Z | | | | |
| | Manikin | | Children | | | Manikin | | Children | | |
Belt Angle	Mean	SD	Mean	SD	**Delta†**	Mean	SD	Mean	SD	**Delta†**
30	-7.2	8.7	-13.8	16.9	**6.6**	25.4	3.9	29.7	13.8	**-4.3**
54	-6.7	3.0	-15.1	20.3	**8.4**	11.5	4.0	20.8	11.6	**-9.3**
75	-10.5	3.2	-24.0	22.4	**13.5**	0.1	3.7	18.9	11.9	**-18.8**

* Summary statistics for measurements by three investigators.
† Manikin mean minus child mean.

DISCUSSION

This study is the first to develop an anatomically realistic physical representation of a child occupant based on statistical analysis of surface measurement data, and the first to develop a belt-fit test device specifically for aviation seating. The manikin and associated test procedures produced good repeatability and reproducibility in belt-fit measurement.

The child posture and belt fit measurement were challenging due to the behavioral independence of toddlers. Nonetheless, the data are meaningful because high postural variability is an important characteristic of this application domain: children in aircraft will assume a wide range of postures and a good restraint system will be robust to those differences. A primary concern with lap belt fit on small children is that the belt will bear on the abdomen rather than the pelvis. However, the belt was overlying the pelvis by at least half the belt width of 48 mm about half the time, and the belt was overlying the pelvis to some extent (i.e., lap belt score Z less than 48 mm) in nearly all cases. Note that the test protocol was such that extreme postures and belt fit were not obtained, so these results do not represent the full spectrum of belt fit that would be expected in the field. Belt fit on the children was significantly affected by lap belt angle but the differences were not large compared to within-condition variance.

The harness tended to pull the lap belt up, potentially increasing the risk of the child sliding down, out of the belt, or being injured by belt loads to the abdomen. However, the harness also constrained torso postures, as expected, and would have better retention in some dynamic events.

The safety outcomes of the range of belt fit observed are unknown. No appropriate surrogate exists for dynamic evaluation of two-year-old children. The ATDs of similar size (12 mo and 3YO) do not have sufficient flexibility to achieve most of the observed postures, and do not have realistic geometry or material properties in the belt-interaction areas. Computational simulation using finite-element modeling is a promising approach for understanding how children of various sizes would respond in a range of dynamic situations. Future work should address these issues to quantify the relationships between static belt position and dynamic restraint performance.

The study is limited by the range of test conditions. Only a single aviation seat configuration, belt, and harness were used. Children were minimally clad and continuously supervised by a caregiver. Testing was conducted over short durations, typically only a few minutes. Accurately locating the ASIS on a young child is challenging, and the measurements led to movements in some cases that added variability to the belt-fit estimates.

Caregivers placed the belt on the child and pulled snug following instructions given by the investigators to ensure good belt placement given the posture of the child. This procedure so that the data would demonstrate the best belt fit that could reasonably be achieved by a conscientious caregiver. Of course, belt fit can be arbitrarily bad, depending on the child's posture and belt-donning procedure. Because the belt lacks a retractor, the level of snugness is determined by the posture and the belt-tightening procedure (and can be affected by subsequent posture change).

The data gathered in this data are appropriate for a range of future studies. The posture data can be used to quantify the distribution of child occupant postures under these scenarios. The manually measured landmark data, which can be used to construct a skeletal linkage defining the

posture. One intriguing possibility is using these data to train automatic posture-tracking software based on depth cameras such as Microsoft Kinect. In previous work, we've developed a system to track the postures of older children; this could be extended to gather naturalistic data on how children behave in aviation settings.

The body shape data have a wide range of potential applications beyond belt fit assessment. The data were gathered in such a way that they can be used to augment the toddler model developed by Kim et al. (2015) and used for the creation of the manikin. Adding posturing capability to the model could extend its application to a wider range of safety assessments. Using methods developed at UMTRI, computational models of children and adults can be rapidly morphed to any body size (Hwang et al. 2016).

Extension of the current work to aviation seat assessments will require some additional effort to develop and test a more formalized measurement procedure. Testing should be conducted with a wider range of seats and installers, and acceptance criteria need to be established. This process should take place in a manner that ensures industry consensus and rapid adoption.

REFERENCES

Hwang, E., Hu, J., Chen, C., Klein, K., Miller, C.S., Reed, M.P., Rupp, J.D., and Hallman, J. (2016). Development, evaluation, and sensitivity analysis of parametric finite-element whole-body human models in side impacts. *Stapp Car Crash Journal*, 60:473-508.

Kim, K.H., Jones, M.L.H., Ebert, S.M., Malik, L., Manary, M.A., Reed, M.P., and Klinich, K.D. (2015). Development of Virtual Toddler Fit Models for Child Safety Restraint Design. Technical Report UMTRI-2015-38. University of Michigan Transportation Research Institute, Ann Arbor, MI.

Park, B-K and Reed, M.P. (2015). Parametric body shape model of standing children ages 3 to 11 years. *Ergonomics*, 58(10):1714-1725. 10.1080/00140139.2015.1033480

Park, B-K D., Ebert, S., and Reed, M.P. (2017). A parametric model of child body shape in seated postures. *Traffic Injury Prevention*. 18(5):533-536. 10.1080/15389588.2016.1269173

Reed, M.P., Ebert-Hamilton, S.M., Klinich, K.D., Manary, M.A., and Rupp, J.D. (2008). Assessing Child Belt Fit, Volume I: Effects of Vehicle Seat and Belt Geometry on Belt Fit for Children with and without Belt Positioning Booster Seats. Technical Report UMTRI-2008-49-1. University of Michigan Transportation Research Institute, Ann Arbor, MI.

Reed, M.P., Ebert-Hamilton, S.M., Klinich, K.D., Manary, M.A., and Rupp, J.D. (2008). Assessing Child Belt Fit, Volume II: Effects of Restraint Configuration, Booster Seat Designs, Seating Procedure, and Belt Fit on the Dynamic Response of the Hybrid-III 10-year-old ATD in Sled Tests. Technical Report UMTRI-2008-49-2. University of Michigan Transportation Research Institute, Ann Arbor, MI.

Reed, M.P., Ebert, S.M., Sherwood, C.P., Klinich, K.D., and Manary, M.A. (2009). Evaluation of the static belt fit provided by belt-positioning boosters. *Accident Analysis and Prevention*, 41:598-607.

Reed, M.P., Ebert-Hamilton, S.M., Klinich, K.D., Manary, M.A., and Rupp, J.D. (2013). Effects of vehicle seat and belt geometry on belt fit for children with and without belt positioning booster seats. *Accident Analysis and Prevention*. 50:512-22. 10.1016/j.aap.2012.05.030

Reed, M.P. (2013). Development of Anthropometric Specifications for the Warrior Injury Assessment Manikin (WIAMan). Technical Report UMTRI-2013-38. University of Michigan Transportation Research Institute, Ann Arbor, MI

Snyder, R.G., Schneider, L.W., Owings, C.L., Reynolds, H.M., Golumb, D.H., and Schork, M.A. (1977). Anthropometry of Infants, Children, and Youths to Age 18 for Product Safety Design. Final Report UM-HSRI-77-17. University of Michigan Transportation Research Institute, Ann Arbor, MI.

Instructions for most standard airplane seats

Figure 1

On seats where the tray table is stowed flat against the seat back (not recessed), as shown in Figure 1, the CARES restraint must be installed under the tray table and can be used for the duration of the flight.
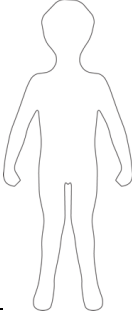
Step 1

Step 2

Step 3

Step 4

Step 5

Kids Fly Safe
CARES®Airplane Safety Harness
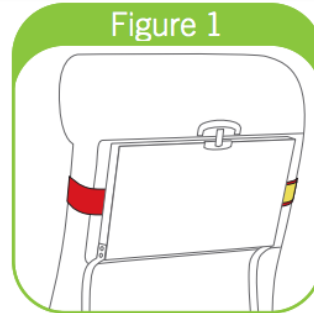
It is acceptable for the buckle to end up at one side instead of between the shoulder straps of the CARES airplane safety harness.

APPENDIX B
SCANNING PROCEDURES

Scan and re-scan until you get a symmetric as close to adult posture for T2 and L1
Take photos

Standing Postures

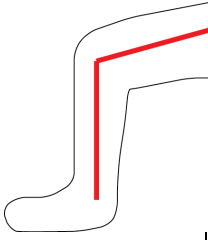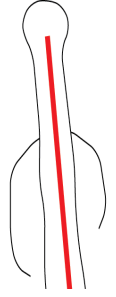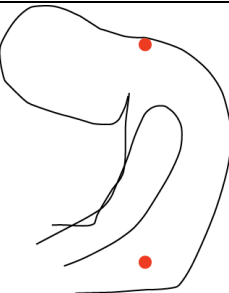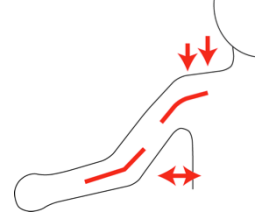|	Legs		Arms	File Name
T2	Feet apart on lines Knees apart		Arms abducted 40˚	VT2 ☐ Scan # Use:
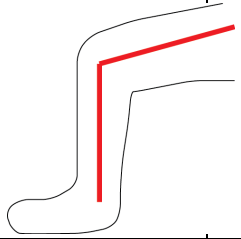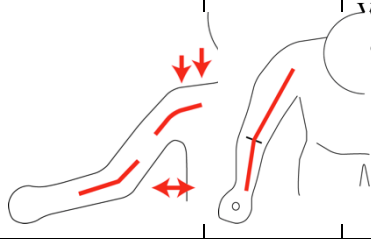
- Make ✔ if completed and note which scan is the best
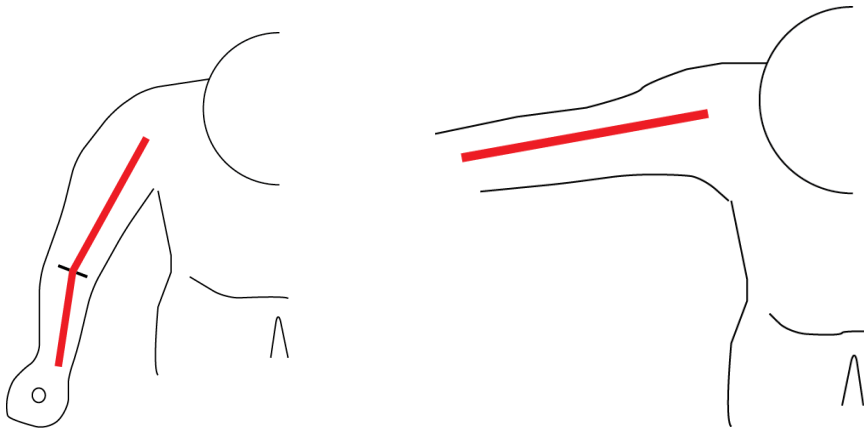
Possible "arm away" Postures as seen from above: left is our scanning standard, right is a way to support the arm against the reconfigurable seat back- also easier to achieve bilateral symmetry with some participants.

Both should have a relaxed shoulder- not raised up towards ears, and elbow with some flexion

In Pedestal Seat (natural back) or Reconfigurable if Child Needs Stability

	Legs			Arms			File Name
L1	Splay: NONE Thigh angled down Ankle under knee			Away			VL1 ☐ can # Use:
AY	Splay: NONE Thigh angled down Ankle under knee			Shoulder: 180˚ flexion with arms away from head "Y" Palms: facing each other			VAY ☐ Scan # Use:
V2	L1	Entire spine in maximum flexion			Away		VV2 ☐ Scan # Use:

42

APPENDIX C
Belt Fit Measurement Procedure

1) Prepare manikin
   Set on flat surface
   - a. Thighs rotated all the way closed
   - b. Rotate head down (chin to chest)
2) Prepare seat and coordinate system
   - a. Measure centerline of the seat
   - b. Set coordinate system relative to centerline plane of the seats
   - c. Rest seat
   - **d.** Cover seat with a muslin cloth or other friction standardizer/reducer (photos below do not include the cloth so that the seat surface is visible)
   - e. Set anchorage position
3) Install Manikin
   - a. Set Manikin on seat surface approximately ½ inch away from seat back
   - b. Keep thighs rotated closed
   - c. Move Manikin until buttocks or back just touches seat back
   - d. Check that the Manikin is centered in the seat – lateral (Y) and rotation around X and Z
   - e. Load manikin with 50 N of force parallel to the floor at PS mark on the pelvis
   - f. Check that the Manikin centerline plane is coincident with centerline plane of the seat
   - g. Place 9.8 kg lead shot bag on thighs.
   - h. Hold thighs down by pressing on the center of the lead shot bag and load manikin with 60 N of force at the torso load point in a direction normal to manikin
   - i. Check that the Manikin centerline plane is coincident with centerline plane of the seat
   - j. Rotate head backward until the head is level. If the head touches the seat back before it is level, stop. The head is level when the intersection/seam between the front and back sections of the head is vertical.
   - k. Remove weight from thighs.
4) Check Installation and Digitize Posture
   - a. Digitized manikin and check that the centerline is coincident with the centerline of the seat.
   - b. If all are within 2 mm, continue. If all are with in 4 mm adjust until symmetrical. If one is => 5 repeat installation.
   - c. Record point list
5) Apply Restraint
   - a. Lap Belt
     - i. Loosen belt until buckle is at end of webbing
     - ii. Buckle
     - iii. Pull slack until webbing is at knees
     - iv. Hold buckle at the height of the top the thighs and tighten belt pulling in the direction of the anchorage
     - v. Pull until snug, but not moving the manikin
   - b. Harness
     - i. Loosen harness adjusters to most loose position
     - ii. Place seat strap around seat so that the bottom of the strap is at the height of the shoulder reference point
     - iii. Thread vehicle belt through harness

iv. Buckle the belt and in the same way as above.
v. Move the harness to…
vi. Tighten the harness until no one cannot pinch the belt, but the tightening does not move the ATD
6) Digitize Belt or Harness and Additional ATD Points
    a. Point list in spread sheet
7) Remove the Belt or Harness and Redigitized ATD Points
    a. Remove the belt or harness, careful not to move the ATD
    b. Re-digitize the manikin point list, as the manikin may have moved during the application of the belt
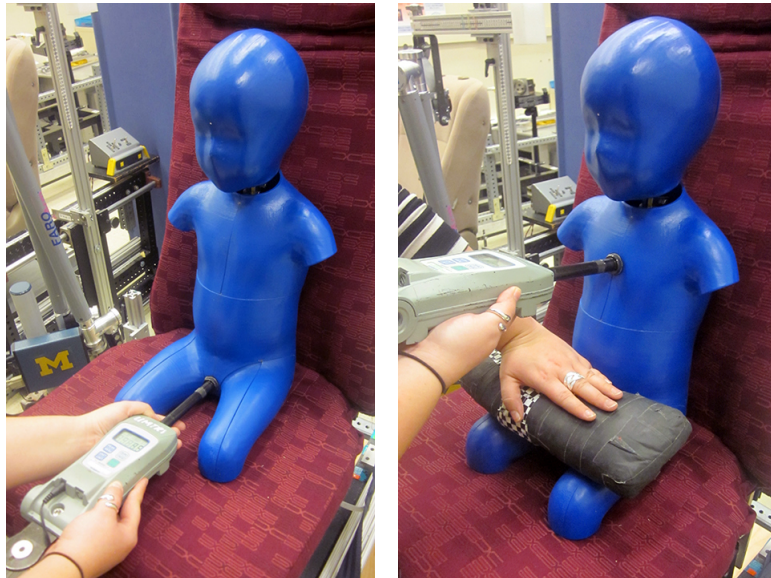

Figure C1. Investigator applying 50 N on pelvis and 60 N on sternum
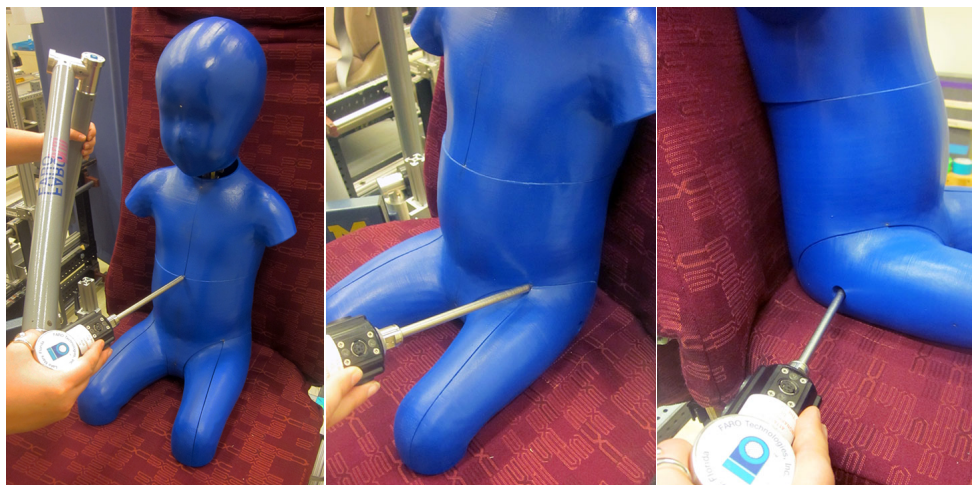

Figure C2. Digitizing points on ATD

Figure C3. Investigator applying lap belt

Figure C4. Digitizing belt location